sciendo

Civil and Environmental Engineering
Vol. 20, Issue 1, 411-425, DOI: 10.2478/cee-2024-0032

EXPERIMENTAL, ANALYTICAL, AND NUMERICAL EVALUATION OF BRIDGE PIER SCOURING

Gouri KADAM[1,*], Balkrishna DAWARI[2]

[1] Research Scholar, Civil Engineering Department, COEP Technology University, Pune, India.
[2] Associate Professor, Civil Engineering Department, COEP Technology University, Pune, India.
[*] corresponding author: gouri.kadam@gmail.com, gk15.civil@coeptech.ac.in

Abstract

Due to the rising number of incidents of bridge failure, scouring around bridges has received a lot of attention. Accurate scour depth prediction is a challenge for researchers and experts, despite massive global research efforts. Estimation the scour depth is crucial for both a safety and economy. Numerous factors affect the scour depth. In this work, the scour depth of three distinct pier geometries – circular, oblong, and rectangular – is thoroughly investigated, and the effect of water depth and discharge on the scour depth of a given geometry is evaluated. Three pier shapes were the subject of a total of 27 trials, nine of which combined three discharges with varying flume water depth. Experimental observation of scour depth shows good agreement with analytical and numerical scour depth values. A comparative examination of analytical, experimental, and numerical findings indicates that numerical models can effectively estimate scour depth, offering a cost-effective and time-saving methodology. Results showed that circular and oblong pier geometry shows lesser scour depth than rectangular pier geometry for a specific combination of flow depth and discharge. Scour depth decreased with increasing flume water depth for the same discharge. For the constant flume water depth, higher discharge results in greater scour depth.

Keywords:

Scour depth;
Local scour;
Bridge pier;
Shape;
Numerical methods.

1 Introduction

Bridges spanning river courses are susceptible to failure due to scour, a complex phenomenon influenced by multiple hydraulic and geometric parameters. Scour study is important from many aspects of bridge safety and stability for scour protection design, risk mitigation, and environmental and hydrological impact assessment. Underestimations of scour depth can affect the safety of the bridge, while over-estimation may lead to an increase in the cost of the substructure. Thus, an accurate estimation of scour depth becomes very important.

Lowering of the bed surface near the vicinity of the bridge pier is termed as scouring. It occurs mainly due to the formation of a horseshoe vortex in front of the pier. Due to this vortex formation, the bed material dislocates and results in scouring. Scouring can drastically impact the hydraulic structure, exposing the foundation which is a common cause of bridge failure worldwide. With the predicted increase in climate extremes due to climate change, the flooding of waterways is expected to rise, and the subsequent scour-related failure of hydraulic structures is likely to increase [1].

Three types of flow scouring were developed, mainly down flow at the face of the pier, the horseshoe vortex at the base of the pier, and the wake vortices formed in the downstream direction of the pier. The formation of the horseshoe vortex and the associated downflow around the bridge element results in increased shear stress and an increase in the sediment transport capacity of the flow. This leads to the development of a deep hole (scour hole) around the bridge element. The formation of the scour hole again changes the flow pattern, causing a reduction in shear stress by the flow and a consequent reduction in the sediment transport capacity.

Scour can occur under any flow condition that makes the bed mobile within the vicinity of the obstruction. It is a soil-structure interaction problem that leads to bed erosion, and subsequently, foundations of the bridge pier, abutments, and riverine structures get exposed [2]. The scour can be classified broadly into two types: general scour and localized (contraction and local) scour. The total

© Author(s) 2024. This work is distributed under the Creative Commons BY 4.0 license (https://creativecommons.org/licenses/by/4.0/).

depth of scour at the bridge foundation (for the pier or abutment) is the sum of the general scour and localized scour [3].

Numerous researchers have conducted parametric studies [4,5] to identify the variables influencing scour depth. This study has enhanced the understanding of flow behavior around the bridge pier in different soil beds, flow depth, and flow velocity. The local scour depth is a function of various flow characteristics, bed material properties, and pier dimensions [6]. Many researchers have carried out experimental study to find out efficient pier geometry, effect of pier characteristics, flow characteristics, bed characteristics and parameters affecting the scour depth [7-12, 20]. In spite of extensive study, designers find it difficult to identify reliable scour depth estimation methodology. Flow intensity is also one of the most important factors affecting the maximum scour depth in local scour [18]. They found that scour depth is depending on many parameters and exactly proportional to the approach flow velocity. Also, lots of efforts in terms of experimental [13,17,22,23,25], analytical [21] and numerical [14-15,20,24] were made towards development of scour depth formula. They found that current scour prediction methods are not suitable as they do not consider the complex nature of the scour formation mechanism. Also, along with experimental studies, scour depth shall be evaluated with numerical and analytical validation and verification studies [13-16]. Along with the traditional experimental studies of scour depth evaluation is also done using neural network methods by Abdussamad [16]. An empirical formula based on the flow depth, mean velocity, critical flow velocity, median grain size and pier diameter was proposed and validated. Hossein [19] carried out a sensitivity analysis of 80 hybrid models of scour depth and critical velocity estimation to find out the most suitable model to find out the efficiency of different equations to determine the critical flow velocity for accurate maximum scour depth estimation around bridge piers. Their study highlighted the use of multiple methodologies as scouring prediction using any one method may be overestimated or underestimated when compared with other methods or observed data. They introduced correction factors in the best-suited equations using regression analysis to decrease the gap between observations and calculated depth. They observed the inverse relationship between pier spacing and scour depth.

Scour depth is influenced by the combined effect of many parameters acting simultaneously on the pier. In India, scour depth estimation is mostly done using empirical formulae as per Indian Road Congress (IRC) guidelines which is developed from Lacey's formula which is based on experimental studies [26]. It's use may lead to incorrect estimation of scour depths leading to uneconomical design. Also, when new river bridge construction on remote sites ceases with a lack of data availability, it becomes difficult to estimate the actual scour depth from bridge safety point of view. Scouring is a complex phenomenon; many parameters such as flow depth, velocity, shape, size of the pier, types of bed materials, angle of attack, etc. affect the scouring depth. Only experimental evaluation may not be sufficient for scour depth estimation within the limited timeframe. It becomes difficult to exactly replicate site conditions in experimental study where numerical modelling plays important role. Current study tries to find out the efficiency of experimental and numerical evaluation methods and compares the scour depth with widely used Colorado State University (CSU) equation. The effect of flow depth, discharge, and shape of the pier on the scour properties evaluated using 27 laboratory experiments. Scour depth then compared with the scour depth formula developed by Colorado State University (CSU) and the numerical simulation carried out using ANSYS fluent software.

2 Experimentation

Experiments were conducted using the tilting flume, 7m long, 0.5m wide, and 0.75m deep, made up of mild steel at the bottom, with the 1.8m test section (Fig. 1) made up of Plexiglas on both sides (Fig. 2). This transparent Plexiglas section helped in the observations and readings. The tank attached to the flume at the entry and the ground storage tank available at the exit was used for recirculation purposes.

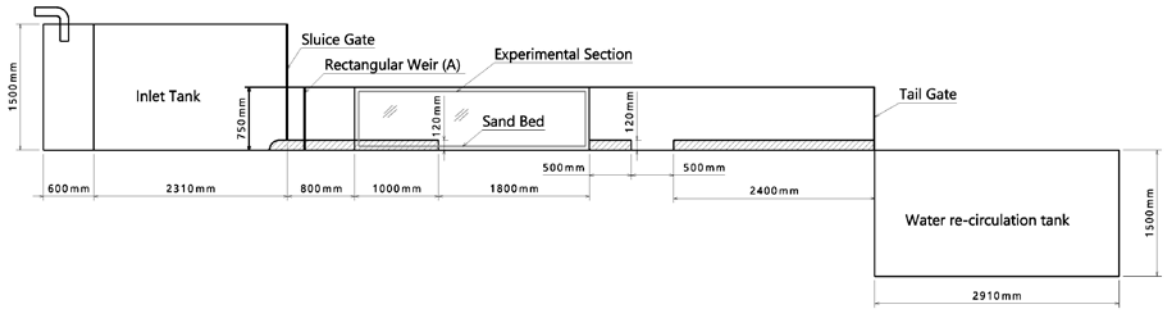

Fig. 1: Longitudinal profile of Laboratory Flume with recirculation tanks.

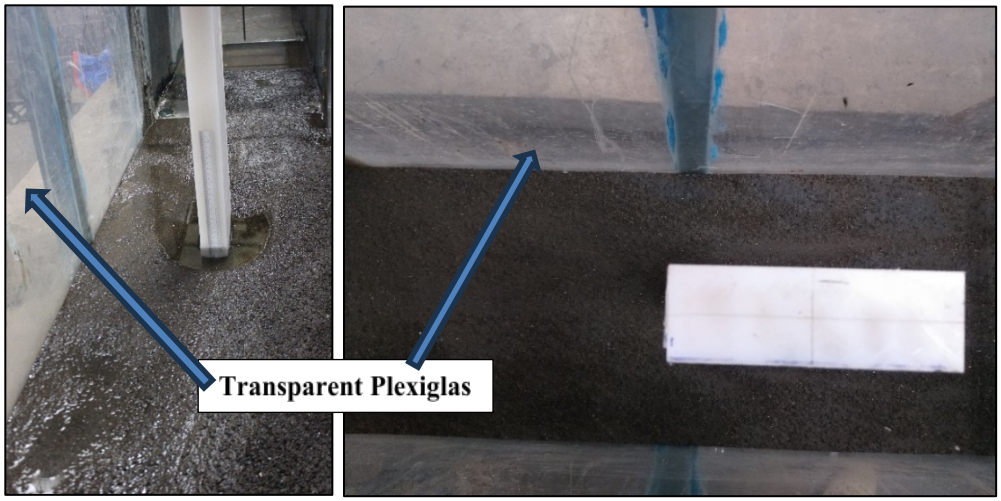

Fig. 2: Experimental section with plexiglass on both sides.

Water was recirculated in the flume with the help of a pump and pipe arrangement placed in the ground storage tank. Discharge from the pump is controlled with the help of the control valve. The flow depth in the flume was controlled with the help of an adjustable tailgate at the downstream end of the flume. The water surface is measured using a point gauge, which is sensitive to the variation of 0.1mm. A rectangular notch (Fig. 3), which was fitted at 0.4m from the sluice gate upstream, was used for discharge measurement using the below formula (1).

$$Q = \frac{2}{3} \times C_d \times L\sqrt{2g} \times H^{\frac{3}{2}} \quad (1)$$

where:
L – Length of the weir,
C_d – Discharge coefficient,
H – Water depth in the notch.

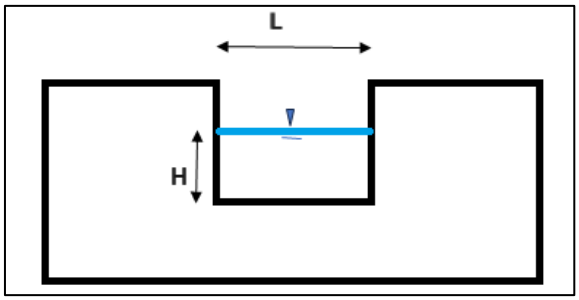

Fig. 3: Rectangular notch.

The existing bed surface was improved by laying a thin layer of sheets, and the bed level was elevated by 0.12m. The sand pit was created 1.8m long 0.5m wide, and 0.12m deep, which was the main test section. Thus, the centre of the pier model is located at 2.3m from the notch. This sand pit is filled with river sand with a median sediment diameter of d_{50}, 1.01mm, and a geometric standard deviation of 1.635. To avoid the turbulence of water at the entry-level, a false bed was tapered at the entrance, and the honeycomb structure was kept vertically at the entrance. Scoured sediments are trapped in rectangular ditches of 0.4m in length provided downstream. Due to this, scoured sand will not reach the recirculation tank and ultimately will not enter a centrifugal pump.

To minimize the effect of side walls on the scour at the pier, the flume width/pier diameter is kept at less than 6.25 [30]. Three pier models (Figs. 4 and 5), circular with 50mm diameter and rectangular with 50x150 mm size and oblong with total 150 mm length, including two half circles with 50 mm diameter at both ends were used for this experiment, thus keeping the width of the exposed surface the same for both shapes. The flume width to pier width ratio was enough to accommodate the flow pattern and scouring effects around the pier. The average depth of water to pier width ratio is always kept greater than 1.5 [11] and the angle of attack of flow is always kept zero during all 27 experiments. After continuously simulating and monitoring scour depth at regular intervals, it was noticed that the depth remained nearly constant throughout the 4-hour experiment. So, the 4-hour time duration was fixed for the following sets of experiments. Nine sets of experiments were conducted with three different water depths in the flume viz 10,11 and 12 cm and three different discharges 17,18 and 20 lit/sec for each pier geometry. Thus, for three pier geometries, a total of 27 experiments were conducted.

Fig. 4: Photo of pier models with rectangular notch.

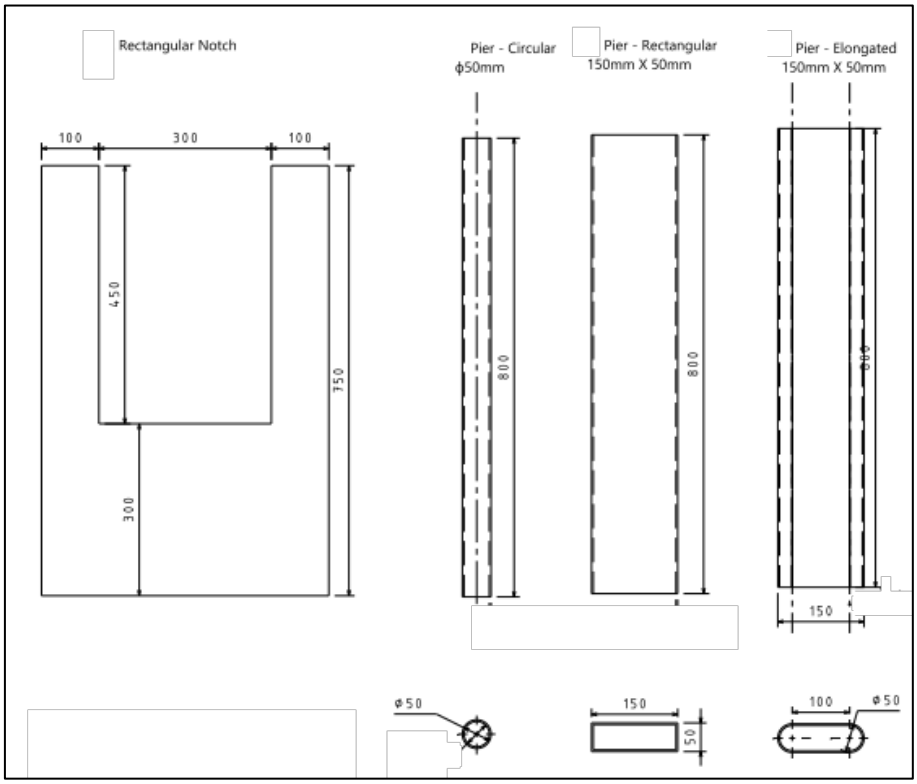

Fig. 5: Pier models with rectangular notch.

2.1 Experimental boundary conditions

Table 1: Summary of 27 experimental conditions for 3 pier shapes.

	D	Q	A	Uc	u^*/u^*_{cr}	Uavg/ Uc	Re	Fr
Pier Model	**Flume Water depth in m**	**Discharge**	**Area = D*0.5**	**Critical Avg velocity**			**Reynold's number**	**Froude number**
		m^3/sec	**m^2**					
Circle	0.1	0.017	0.05	0.38	0.634	0.895	33885	0.343
Ø 0.05m	0.11	0.017	0.055	0.386	0.655	0.801	33875	0.297
	0.12	0.017	0.06	0.391	0.676	0.724	33845	0.261
	0.1	0.018	0.05	0.38	0.634	0.947	35878	0.363
	0.11	0.018	0.055	0.386	0.655	0.847	35848	0.315
	0.12	0.018	0.06	0.391	0.676	0.767	35878	0.277
	0.1	0.02	0.05	0.38	0.634	1.053	39864	0.404
	0.11	0.02	0.055	0.386	0.655	0.943	39904	0.35
	0.12	0.02	0.06	0.391	0.676	0.852	39825	0.307
Rectangular	0.1	0.017	0.05	0.38	0.634	0.895	33885	0.343
b = 0.05m	0.11	0.017	0.055	0.386	0.655	0.801	33875	0.297
	0.12	0.017	0.06	0.391	0.676	0.724	33845	0.261
	0.1	0.018	0.05	0.38	0.634	0.947	35878	0.363
	0.11	0.018	0.055	0.386	0.655	0.847	35848	0.315
	0.12	0.018	0.06	0.391	0.676	0.767	35878	0.277

	D	Q	A	Uc	u*/u*$_{cr}$	Uavg/ Uc	Re	Fr
	0.1	0.02	0.05	0.38	0.634	1.053	39864	0.404
	0.11	0.02	0.055	0.386	0.655	0.943	39904	0.35
	0.12	0.02	0.06	0.391	0.676	0.852	39825	0.307
Oblong	0.1	0.017	0.05	0.38	0.634	0.895	33885	0.343
b = 0.05m	0.11	0.017	0.055	0.386	0.655	0.801	33875	0.297
	0.12	0.017	0.06	0.391	0.676	0.724	33845	0.261
	0.1	0.018	0.05	0.38	0.634	0.947	35878	0.363
	0.11	0.018	0.055	0.386	0.655	0.847	35848	0.315
	0.12	0.018	0.06	0.391	0.676	0.767	35878	0.277
	0.1	0.02	0.05	0.38	0.634	1.053	39864	0.404
	0.11	0.02	0.055	0.386	0.655	0.943	39904	0.35
	0.12	0.02	0.06	0.391	0.676	0.852	39825	0.307

Fig. 1 shows the longitudinal profile of the flume. River sand is filled in an experimental section with dimensions 1.8m X 0.5m X 0.12 m. Table 1 shows the parameters used during experimental simulation. Horse shoe vortex phenomenon which is mainly responsible for scouring is governed by Froude number and flow characteristics are determined from Reynold's number. Reynolds number and Froude number helps in determining the flow behaviour, depth of flow. Flow intensity ratio, the ratio of maximum shear velocity (**u***) to critical shear velocity (**u*$_{cr}$**) varies from 0.634 to 0.676. The ratio of pier diameter (or width) to the width of the channel is kept below 15% to avoid the effect of boundary shear on the local scour development [30]. The pier diameter is selected in such a way that the ratio of pier diameter to d_{50} is kept at more than 25 to avoid the coarseness effect [11].

Critical shear stress and other parameters were calculated using Shield's curve and [29] method, as mentioned in Equations 2 to 5.

$$D_* = D_{50}\left[\frac{(s-1)g}{\upsilon^2}\right]^{1/3} \tag{2}$$

$$\theta_{cr} = \begin{cases} 0.24{D_*}^{-1} & D_* \leq 4 \\ 0.14{D_*}^{-0.64} & 4 < D_* \leq 4 \\ 0.24{D_*}^{-0.10} & 10 < D_* \leq 20 \\ 0.013{D_*}^{-0.29} & 20 < D_* \leq 150 \\ 0.055 & 150 < D_* \end{cases} \tag{3}$$

$$\frac{U_c}{{U^*}_c} = 5.75log\left(5.53\frac{h}{D_{50}}\right) \tag{4}$$

$${u^*}_{cr} = \sqrt[2]{(s-1)gD_{50}\theta_{cr}} \tag{5}$$

where:

D_* – Particle diameter,
D_{50} – Median sediment diameter in mm,
s – Specific gravity,
υ – Kinematic viscosity,
h – Water depth in the flume,
θ_{cr} – Critical Shields number (dimensionless),

U_c – Critical average velocity [m/sec],
U^*_c – Critical average shear velocity [m/sec],
u^*_{cr} – Critical shear velocity,
u^* – Maximum shear velocity = $\sqrt[2]{gRS}$,
R – Hydraulic radius,
S – Slope of the channel,
Q – Discharge.

3 Numerical scour depth evaluation

The observed scour depth is compared with the numerical scour depth. CFD model was created for all three pier geometries. The experimental section was exactly modelled in ANSYS to replicate the same model and boundary conditions i.e., from the sluice gate at the entry level to the tailgate placed at the exit along with the sand bed with a depth of 0.1m (Fig. 5). The simulation is carried out for flow rates and water depths same as used in the experimental analysis. The water flow is modelled as incompressible and turbulent. The ICEM CFD tool is used to generate the geometry and mesh. The generated mesh is structured, resulting in maximum accuracy due to minimal skewness (Fig. 6). The simulation is carried out using the fluent solver. For CFD modeling, the multiphase Eulerian model approach is used. The simulation is transient, with a total time step of one second to keep the simulation stable.

The velocity inlet condition is provided for the inlet and outlet boundary total pressure outlet boundary condition. The boundary condition for the wall is no slip. Continuity, momentum, and energy equations were solved. The velocity contour was plotted for all the 27 experimental combinations. One of the contour plots developed for discharge 0.017 m^3/sec and water depth 0.11m is shown in Fig. 7.

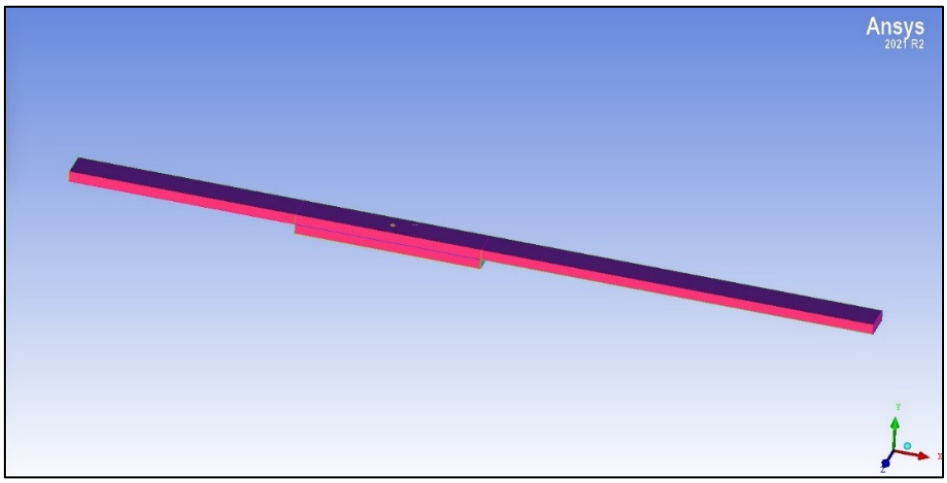

Fig. 6: Computational Domain considered for CFD analysis.

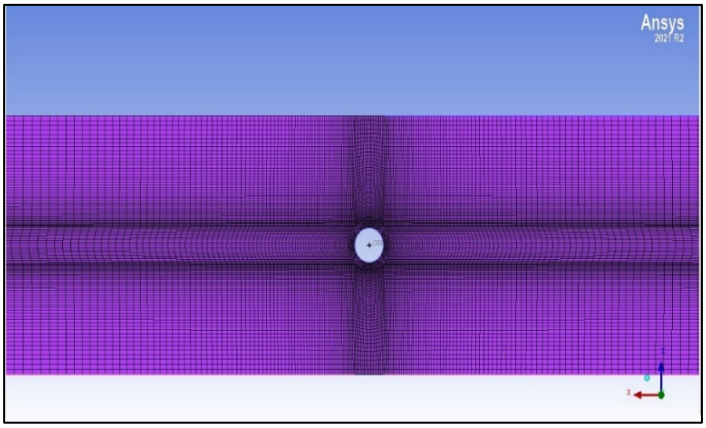

Fig. 7: Structured Mesh generated around the pier.

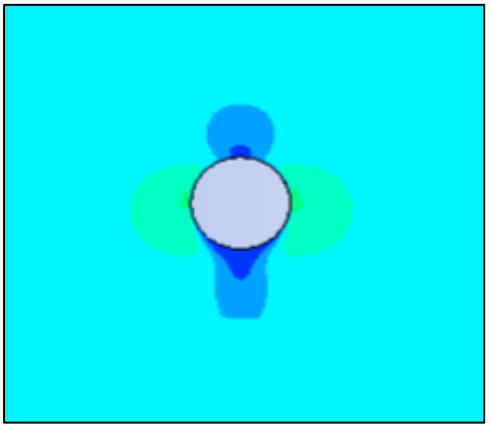
Fig. 8: Velocity contour with discharge 0.017 m^3/sec and water depth 0.11m.

3.1 Governing Equations

The numerical model used solves the incompressible Reynolds-averaged Navier -Stokes equations. Governing equations of the flow are continuity and momentum equations.

Continuity equation:

$$\frac{\partial U}{\partial x} + \frac{\partial V}{\partial y} + \frac{\partial W}{\partial z} = 0 \tag{6}$$

Momentum equation:

$$\frac{\partial U}{\partial t} + U.\nabla U = -\frac{1}{\rho}\frac{\partial P}{\partial x} + \nabla.(\nu \nabla U) - \frac{\partial}{\partial x}(\underline{u'^2}) - \frac{\partial}{\partial y}\underline{(u'v')} - \frac{\partial}{\partial z}\underline{(u'w')} \tag{7}$$

$$\frac{\partial V}{\partial t} + V.\nabla V = -\frac{1}{\rho}\frac{\partial P}{\partial y} + \nabla.(\nu \nabla V) - \frac{\partial}{\partial x}(\underline{v'u'}) - \frac{\partial}{\partial y}\underline{(v'^2)} - \frac{\partial}{\partial z}\underline{(v'w')} \tag{8}$$

$$\frac{\partial W}{\partial t} + W.\nabla W = -\frac{1}{\rho}\frac{\partial P}{\partial z} + \nabla.(\nu \nabla W) - \frac{\partial}{\partial x}(\underline{w'u'}) - \frac{\partial}{\partial y}\underline{(w'v')} - \frac{\partial}{\partial z}\underline{(w'^2)} \tag{9}$$

Energy equation:

$$\rho C_p \frac{\partial T}{\partial t} + \rho U_j C_p \frac{\partial T}{\partial x_j} = \frac{\partial}{\partial x_j}[\lambda_{eff}\frac{\partial T}{\partial x_j} - \rho C_p(u_j'T')] \tag{10}$$

Where, u, v, w, ρ are the instantaneous values and U, V, W, P are the mean values and u', v', w' are the fluctuating part. The instantaneous variables in the Naiver-Stokes equations are replaced by the mean and fluctuating part and simplified through a process called Reynolds averaging where the unsteadiness of the flow is removed through time-averaging. Equation 6 represents the conservation of mass and equations 7 to 9 correspond to conservation of momentum in X, Y and Z directions, where:

$$u = U + u'v = V + v'w = W + w'p = P + p' \tag{11}$$

Equation 10 represents the energy equation. The wall shear stress, τ_w is given by Equation 12:

$$\tau_w = \mu\left(\frac{\partial u}{\partial y}\right) y = 0 \tag{12}$$

Where μ is the dynamic viscosity, u is the flow velocity parallel to the wall and y is the distance to the wall. The SI unit of the wall shear stress is pascal (Pa).

4 Analytical scour depth evaluation

Indian Road Congress, IRC 1998 & 2000 [27] is using equation (13) for calculating scour depth based on the formula derived by Lacey-Inglis [26].

Mean depth of scour:

$$d_{sm} = 1.34(q^2/f)^{1/3} \tag{13}$$

where:

Q – Design discharge in cumecs,

Q – Discharge intensity i.e. $m^3/s/m$ i.e. $\frac{Q}{L}$,

F – Lacey's silt factor given by equation $1.76(d_m)$ ½,

d_m – Weighted mean diameter of sand,

L – Clear waterway under the bridge.

The CSU (Colorado State University) [28] equation (14) is a commonly used empirical formula for estimating scour depth around bridge piers in river environments. CSU equation is solved for scour depth calculation of the present experimental study of all 27 experiments. The purpose of this investigation is to assess the accuracy of the experimental evaluation with a well-known scour depth prediction equation which considers many parameters affecting to the scour depth compared to other analytical equations.

$$y_s = 2.0K_1K_2K_3K_4a^{0.65}y_1^{0.35}Fr_1^{0.43} \quad (14)$$

where:

y_s – Equilibrium depth of scour,
y_1 – Flow depth at upstream,
a – Pier width,
K_1 – Correction factor for pier nose shape,
K_2 – Correction factor for angle of attack of flow $= \left(cos\theta + \frac{L}{a}sin\theta\right)^{0.65}$,
K_3 – Correction factor for bed condition,
K_4 – Correction factor for armouring of bed material $= 0.4(V_R)^{0.15}$.

5 Results and Discussion

After 4 hours of experiment, water is allowed to drain. A grid with equal distant points covering the maximum extent of scour is plotted around the pier section (Fig. 9d). In Fig. 9 (a, b, c), the shape of the scour whole around the pier geometry due to flow separation is clearly visible. Scour hole is marked in white colour, and the deposition is marked in red colour. Maximum scour depth is observed on the upstream side alongside the face of the pier. Measurements showed that rectangular pier geometry F(Fig. c) shows the maximum scour depth and extent. Also, the amount of deposition at the downstream size is more in rectangular pier geometry. Along with scour depth, extent of scour needs to be considered in scour depth evaluation from bridge safety point of view.

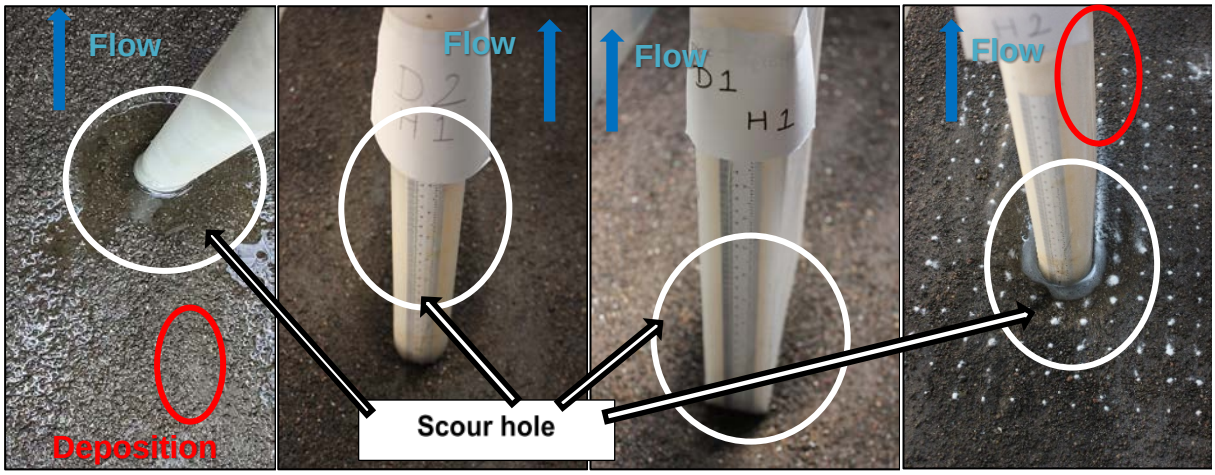

a) Circular. b) Oblong. c) Rectangular. d) Measurement Grid.

Fig. 9: Scour hole generated around the pier models.

For each pier, a total 9 experiments with 3 discharges and 3 flume water depths were carried out. Initially, discharge is kept constant and water depth in the flume is adjusted with tail gate to achieve water depth 0.1(D1), 0.11(D2) and 0.12(D3) m. Discharge is varied slowly to achieve constant discharge from 0.017(Q1) to 0.018(Q2) and finally to 0.02(Q3) m3/sec. After each experiment, scour depth is measured at a predefined grid point location, and contour plots are developed as shown in Fig. 10 (for Circular), Fig. 11 (for Rectangular) and Fig. 12 (for Oblong). It has been observed that when the flow water depth is considered a constant value, scour depth increases with an increase in discharge. The extent of scour shows variation and increases with an increase in discharge value. This can be

visualized while comparing scour depth in one row (e.g., D1Q1, D1Q2 and D1Q3 i.e Fig. a, Fig. b and Fig. c of Fig. 10, 11 and 12 for respective pier geometry.

On the other hand, when discharge is kept constant, a decrease in scour depth is observed with an increase in the water depth of the flume. Also, the extent of the scour decreased with an increase in the depth of water. This can be visualized while comparing scour depth in one column (e.g., D1Q1, D2Q1 and D3Q1 i.e Fig. a, Fig. d and Fig. g of Fig. 10, 11 and 12. For all the pier shapes, maximum scour depth is observed when discharge is maximum, and flow depth is minimum, i.e., D1Q3 (Fig. c of Fig. 10, 11 and 12) and also from Fig. 14 when plotted separately. Rectangular pier geometry shows maximum scour depth compared to circular and oblong pier geometry (Fig. 13). Table 2 shows that the extent of scour depth is more significant for rectangular pier compared to the circular and oblong pier geometry. Fig. 15 shows comparison of scour depth values obtained after experimental evaluation, numerical simulation, and using analytical formulae. It has been seen clearly from the graph that Experimental results are in good agreement [R^2 between 0.69 to 0.93] with the scour depth computed using HEC-CSU formula for Oblong and circular pier geometry. For rectangular pier geometry, experimental and numerical results follow the same trend.

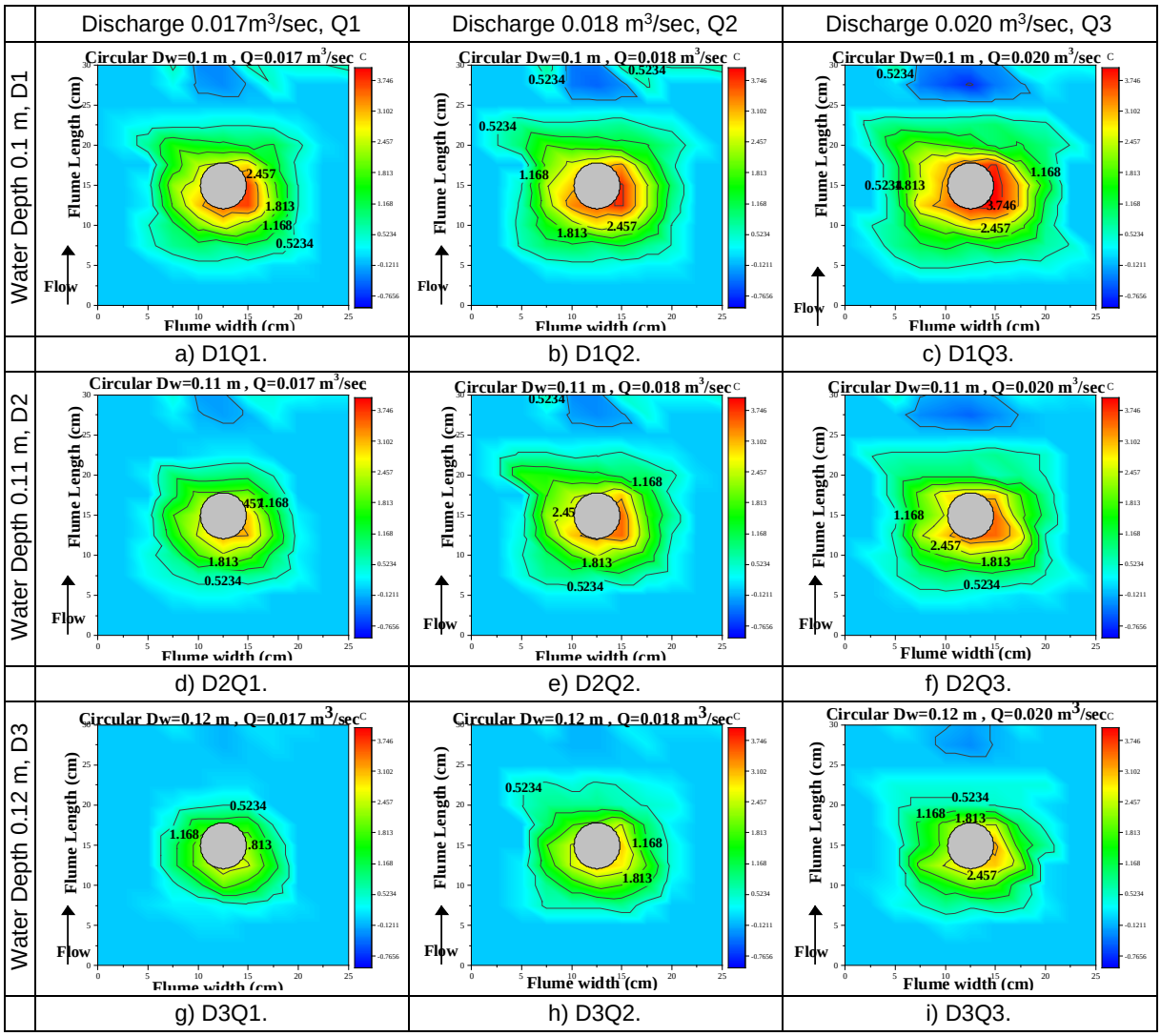

Fig. 10: Scour depth profile around Circular pier.

	Discharge 0.017m³/sec, Q1	Discharge 0.018 m³/sec, Q2	Discharge 0.020 m³/sec, Q3
Water Depth 0.1 m, D1	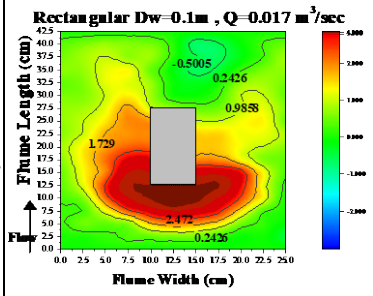	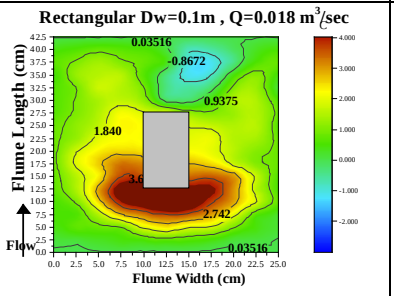	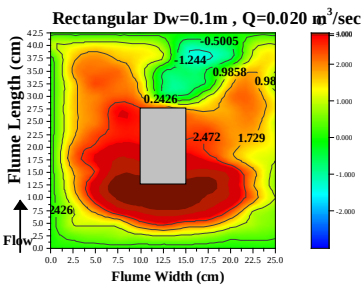
	a) D1Q1.	b) D1Q2.	c) D1Q3.
Water Depth 0.11 m, D2	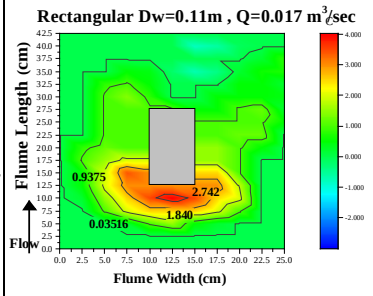	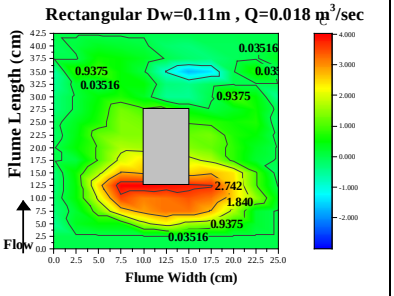	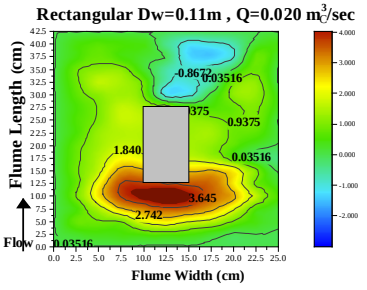
	d) D2Q1.	e) D2Q2.	f) D2Q3.
Water Depth 0.12 m, D3	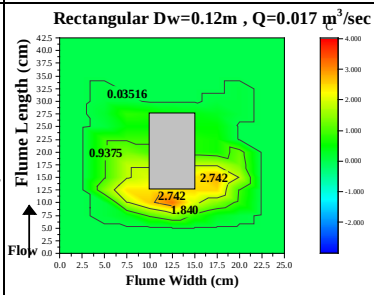	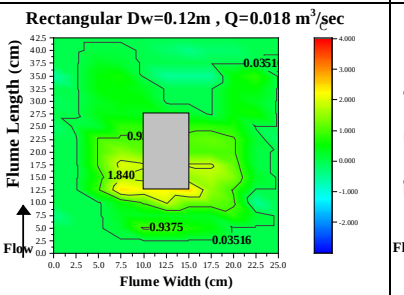	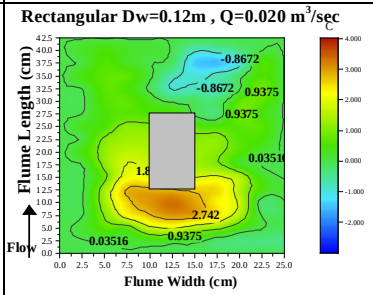
	g) D3Q1.	h) D3Q2.	i) D3Q3.

Fig. 11: Scour depth profile around Rectangular pier.

	Discharge 0.017m³/sec, Q1	Discharge 0.018 m³/sec, Q2	Discharge 0.020 m³/sec, Q3
Water Depth 0.1 m, D1	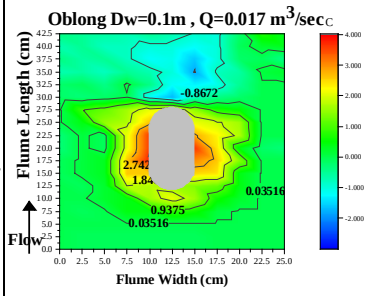	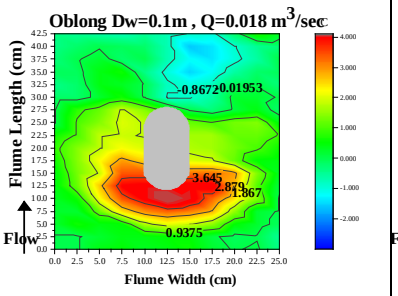	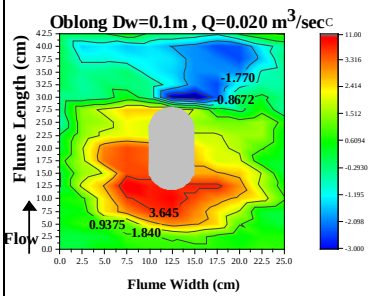
	a) D1Q1.	b) D1Q2.	c) D1Q3.
Water Depth 0.11 m, D2	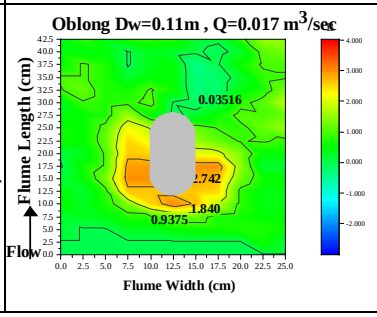	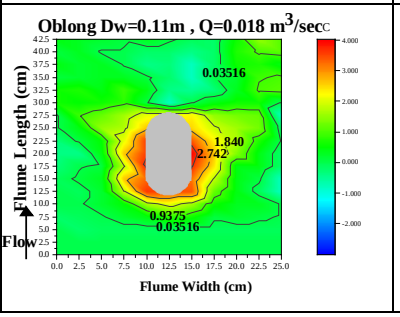	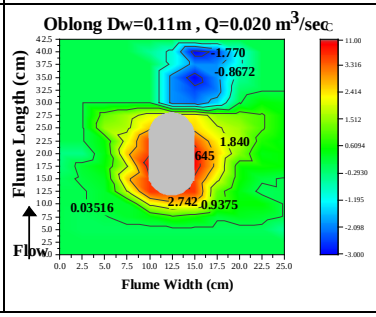	

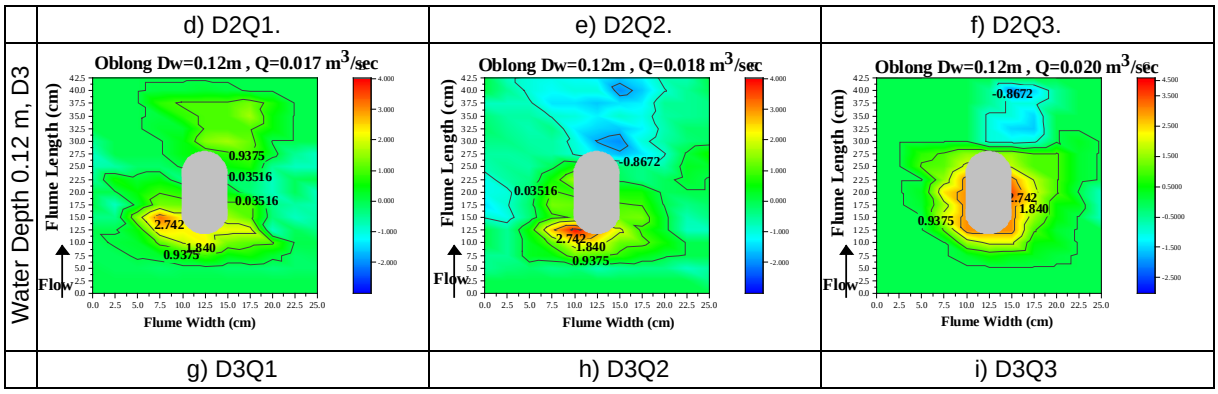

Fig. 12: Scour depth profile around Oblong pier.

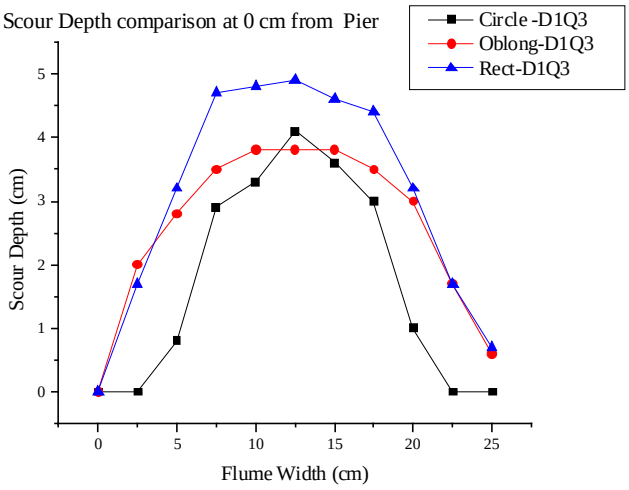

Fig. 13: Scour depth comparison at the pier face centre.

Table 2: Scour geometry parameters for discharge 0.020 m³/sec, depth 0.10m.

Shape of pier		Width/dia [m]	Length/dia of pier [m]	Scour depth [m]	Scour length [m]	Scour width [m]
Circle		0.05	0.05	0.041	0.175	0.150
Rectangle		0.05	0.15	0.05	0.375	0.175
Oblong	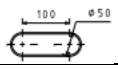	0.05	0.15	0.038	0.263	0.162

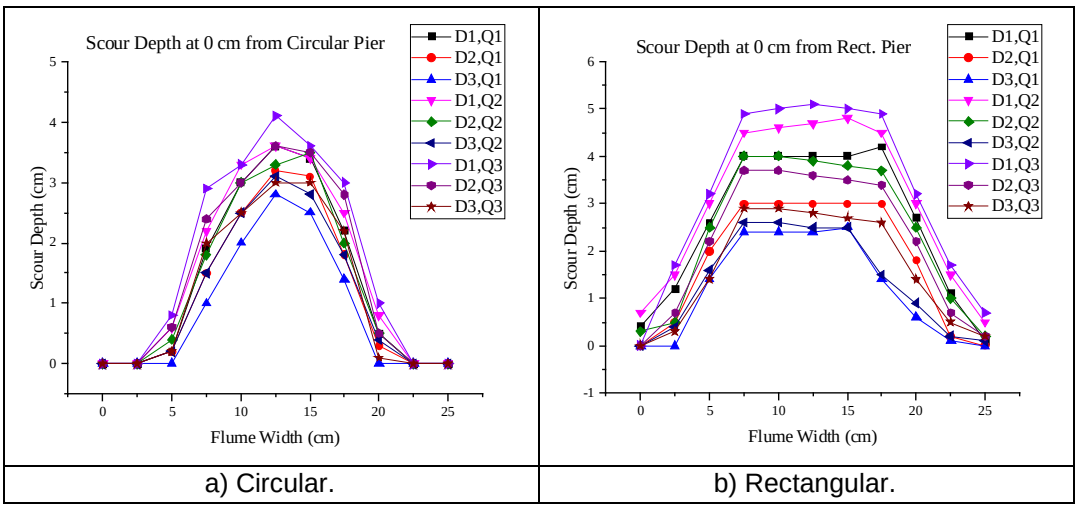

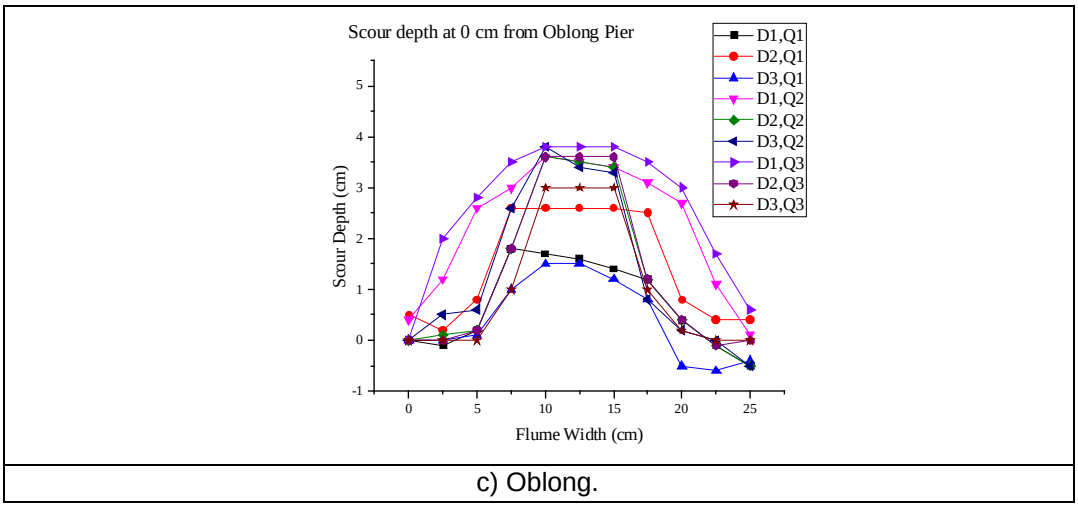

c) Oblong.

Fig. 14: Scour depth at the upstream side of pier face.

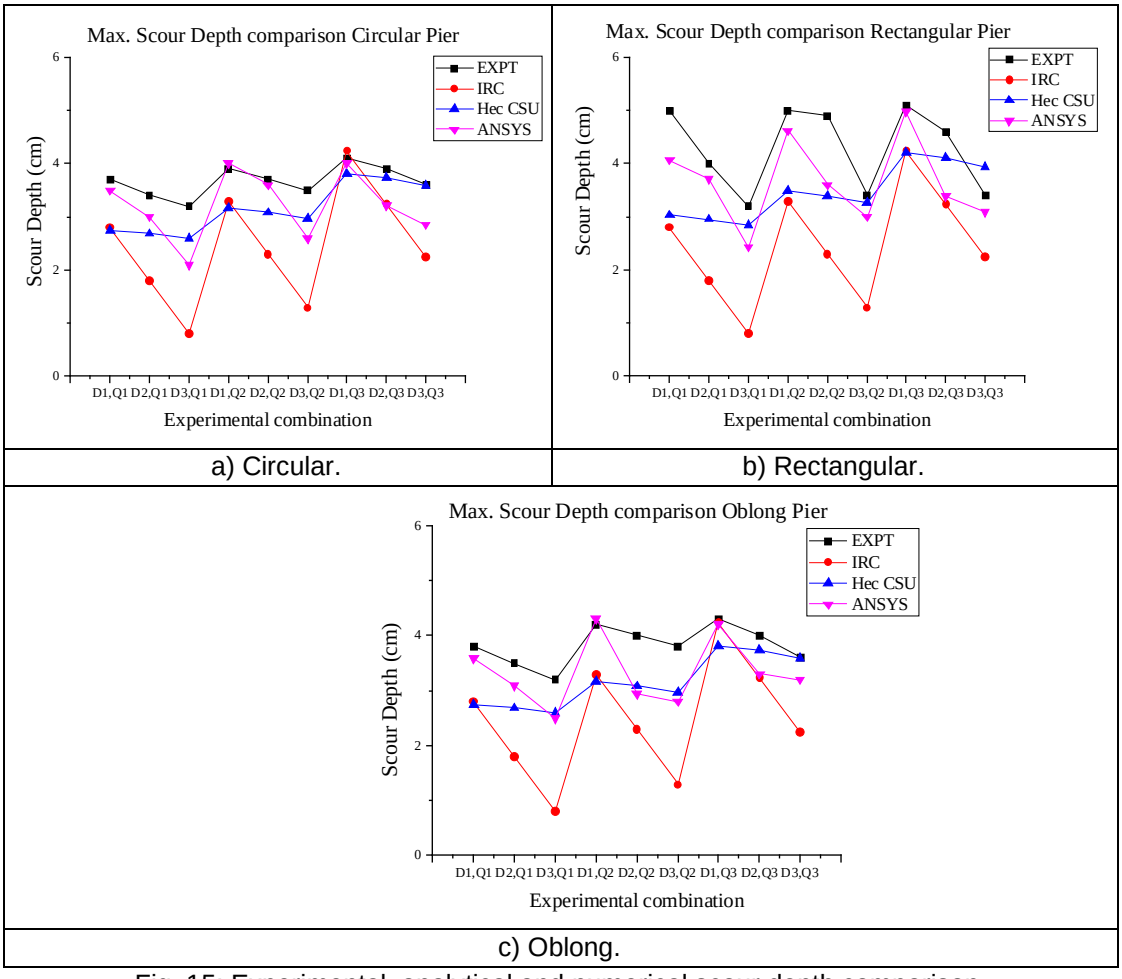

a) Circular.

b) Rectangular.

c) Oblong.

Fig. 15: Experimental, analytical and numerical scour depth comparison.

6 Conclusions

The current study evaluates the integrated effect of parametric influence on scour depth. Effect of discharge, flow depth, and pier shape on scour depth is studied over here. The following conclusions can be drawn from this experimental evaluation:

1) Comparison of experimental, numerical, and analytical results using CSU formula shows good agreement with each other while scour depth using IRC formula shows more variation. Results showed the effectiveness of experiment and numerical methods for actual scour depth estimation. Also, since

experimental simulation is more time consuming, costly and require more manpower, calibrated, and validated Numerical methodology proves to be more useful and effective.

2) Scour depth calculated using IRC equation is same for all the shapes of piers. This highlights the requirement of modifications in IRC equation with respect to inclusion of factors for pier geometry and flow characteristics.

3) It is observed that scour depth is always maximum close to the pier on upstream side than the downstream side. Thus, highlights that scour protection measures shall be implemented more efficiently on the upstream side of pier.

4) Rectangular pier shape shows maximum scour depth and oblong pier shape shows minimum scour depth which agrees well with previous researches. It is observed that as compared to discharge and flow depth, pier geometry has more influence on scour depth which needs to be considered in scour depth evaluation. There is deposition observed on the downstream side which is maximum for rectangular pier.

5) When the discharge is kept constant, for a particular pier geometry scour depth, length and width decreases with an increase in flow depth with a significant reduction in the Froude number. This highlights that the effective channel width also plays an important role in scour depth evaluation.

6) When flow depth is kept constant, for a particular pier geometry scour depth, length and width increases with an increase in discharge with a significant increase in Froude number is observed.

7) It is observed that the length of the pier shape geometry affects the flow pattern around the pier and plays a vital role in determining scour depth on the downstream side and the overall geometry of the scour.

Acknowledgement

I wish to thank my research supervisor for providing the insight and expertise that helped in the research. I would also like to thank my colleagues at COEP technological university who helped directly or indirectly in successful conduction of the experiments.

References

[1] CRASWELL, T - AKIB S.: Reducing Bridge Pier Scour Using Gabion Mattresses Filled with Recycled and Alternative Materials. Eng 2020, 1, pp 188–210; doi:10.3390/eng1020013.
[2] JALAL, H. K. - HASSAN, W. H.: Effect of Bridge Pier Shape on Depth of Scour. IOP Conf. Series, Materials Science and Engineering 2020,671.
[3] KHALID, M. - DANISH, M.: Review of the scour management for mitigating the bridge failure. UKIERI Concrete Congress, 2020 Corpus ID: 219615772.
[4] ABED, B. S. - MAJEED, H. Q.: The Behavior of Scouring Around Multiple Bridge Piers Having Different Shapes. IOP Conf. Series, , Materials Science and Engineering., 2020, 745 012158.
[5] RAJAIE, M. - PIRESTANI, M. R. - ABADI, S. H. G. N.: Effects of Oval and Circular Piers on Velocity and Shear Stress Changes by using Open FOAM Software, Curr. World Environ., Vol. 10(Special Issue 1), 2015,pp 1109-1115. http://dx.doi.org/10.12944/CWE.10.Special-Issue1.130.
[6] MELIAN, Q. - JINZHA, L. - QIGANG, C.: Comparison of existing equations for local scour at bridge piers: parameter influence and validation, Springer Science+Business Media Dordrecht, 2016, DOI 10.1007/s11069-016-2287-z.
[7] FAROOQ, R. - GHUMMAN, A. R.: Impact Assessment of Pier Shape and Modifications on Scouring around Bridge Pier. Water 11, 2019, 1761. doi:10.3390/w11091761.
[8] ELDHO, T. I - VISWANADHAM, B. V. S. - VIJAYASREE, B. A.: Physical Model Study of Scouring Effects on Pier Foundations of Bridges, Indian Geotechnical Conference – 2010, GEOtrendz December 16–18, 2010 IGS Mumbai Chapter & IIT Bombay.
[9] VIJAYASREE, B. A - ELDHO, T. I.: Experimental study of scour around bridge piers of different arrangements with same aspect ratio, Scour and Erosion – Harris, Whitehouse & Moxon (Eds) © 2016 Taylor & Francis Group, London, 2016, ISBN 978-1-138-02979-8.
[10] BARANWAL, A. - DAS, B. S. - SETIA, B.: A comparative study of scour around various shaped bridge pier. Eng. Res. Express 5, 2022, 015052.
[11] VIJAYASREE, B. A. - ELDHO, T. I. - MAZUMDER, B. S. - AHMAD, N.: Influence of bridge pier shape on flow field and scour geometry. International Journal of River Basin Management, 2017.
[12] KADONO, T. - KATO, S. - OKAZAKI, S. - MATSUI, T. - KAJITANI, Y. - ISHIZUKA, M. - YOSHIDA, H.: Effects of Dynamical Change in Water Level on Local Scouring around Bridge Piers Based on In-Situ Experiments. Water, 13, 3015, 2021, https://doi.org/ 10.3390/w13213015.

[13] SAHA, R. - LEE, S. O. - HONG, S. O.: A Comprehensive Method of Calculating Maximum Bridge Scour Depth. Water 2018, 10, 1572; doi:10.3390/w10111572.
[14] OBEID, Z. H. - AL-SHUKUR, A. H.: 3D Numerical Simulation of Local Scouring and Velocity Distributions around Bridge Piers with Different Shapes. AARJMD VOLUME 3 ISSUE 2 (FEBRUARY 2016) ISSN: 2319 – 2801.
[15] BAYON, B. - VALERO, D. - VALLES, F. M. - LOPEZ, P. A. - JIMENEZ: Comparison of CFD Models for Multiphase Flow Evolution in Bridge Scour Processes. 5th International Junior Researcher and Engineer Workshop on Hydraulic Structures Spa, Belgium, 28-30 August 2014.
[16] ISMAIL, A.: Prediction Of Scour Depth Around Bridge Piers Using Evolutionary Neural Network. Mathematical Modelling in Civil Engineering Vol. 14-No. 2: 26-36 - 2018, Doi: 10.2478/mmce-2018-0005.
[17] CHIBANA, T. - QUIOCHO, R. - WATANABE, K.: Role of Grain Size Distribution and Pier Aspect Ratio in Scouring and Sorting around Bridge Piers. Water 2022, 14, 2066. https://doi.org/10.3390/w14132066.
[18] DU, S. - WANG, Z. - WANG, R. - LIANG, B. - PAN, X.: Effects of flow intensity on local scour around a submerged square pile in a steady current, Phys. Fluids 34, 085126 (2022); https://doi.org/10.1063/5.0103556.
[19] HAMIDIFAR, H. - ZANGANEH-INALOO, F. - CARNACINA, I.: Hybrid Scour Depth Prediction Equations for Reliable Design of Bridge Piers, Water 2021, 13, 2019. https://doi.org/10.3390/w13152019
[20] ABED, B. S. - MAJEED, H. Q.: The Behavior of Scouring Around Multiple Bridge Piers Having Different Shapes. IOP Conf. Ser.: Mater. Sci. Eng. 745 012158, 2020.
[21] OMARA, H. - TAWFIK, A.: Numerical study of local scour around bridge piers IOP Conference Series: Earth and Environmental Science, IOP Publishing, 2018, DOI: https://doi.org/10.1088/1755-1315/151/1/012013.
[22] VAGHEFI, M. - GHODSIAN, M. - SALIMI, S.: Scour Formation Due to Laterally Inclined Circular Pier, Arab. J. Sci. Eng. 41 (2016) 1311–1318. doi:10.1007/s13369-015-1920-6.
[23] VAGHEFI, M. - MASOUD, G.: The effect of circular bridge piers with different inclination angles toward, Sadhana. (2015). doi:10.1007/s12046-015-0443-x.
[24] BAYKAL, C. - SUMER, B. M. - FUHRMAN, D. R. - JACOBSEN, N. G. - FREDSØE, J.: Numerical investigation of flow and scour around a vertical circular cylinder. Phil. Trans. R. Soc. A 373: 20140104, 2015, http://dx.doi.org/10.1098/rsta.2014.0104.
[25] MORENO, M. - MAIA, R. - COUTO, L. - CARDOSO, A.: Contribution of complex pier components on local scour depth, 3rd IAHR Europe Congress, Book of Proceedings, 2014, Porto -Portugal
[26] Umesh K.: Indian practice on estimation of scour around bridge piers – A comment. Sadhana Vol. 32, Part 3, June 2007, pp. 187–197.
[27] IRC: 78-2000, Standard specifications and code of practice for road bridges. The Indian Roads Congress, New Delhi, India, 2000.
[28] HEC-18., Evaluating scour at bridges: Federal Highway Administration Hydraulic Engineering Circular No. 18, FHWA, National Highway Institute, USA, 2012, 5th edn.
[29] LEO, C. van RIJN (1984). Sediment Transport, Part III: Bed forms and alluvial roughness. Journal of Hydraulic Engineering, Vol 110.
[30] RAUDKIVI, A. J. - ETTEMA, R.: Clear-water scour at cylindrical piers. Journal of Hydraulic Engineering, Volume 109, Issue 3, 1983.